Optical interferometry imaging from space: optimization of the aperture configuration of a dense array

Hiyam Debary, Laurent Mugnier, Vincent Michau, Sébastien Lopez

Optical interferometry imaging from space: optimization of the aperture configuration of a dense array

Hiyam Debary[a], Laurent M. Mugnier[a], Vincent Michau[b], and Sébastien Lopez[c]

[a]DOTA, ONERA, Université Paris Saclay, 29 Av. de la Division Leclerc, F-92322 Châtillon, France
[b]DSG, ONERA, Université Paris Saclay, 6 Ch. de la Vauve aux Granges, F-91120 Palaiseau, France
[c]Airbus Defence and Space, 31 Rue des Cosmonautes, 31402 Toulouse Cedex 4, France

ABSTRACT

The advent of photonic integrated circuits (PICs) will allow the replacement of the large aperture of an optical telescope by a dense array of small apertures combined interferometically. The light coming from aperture pairs can be combined by a PIC in order to extract interferogram characteristics known as complex visibilities, from which the observed object can then be reconstructed. In such a compact interferometric imager, the optical components dedicated to image formation in a regular telescope are no longer necessary. In particular, such a concept is relevant for space missions where weight and size are critical. To date, the proposed concepts are made of one-dimensional arrays radially disposed in a circular instrument.

The way of combining the apertures defines the optical transfer function of the instrument, which is key to the imaging performance. In this communication, our goal is to optimize the aperture configuration. Signal-to-noise considerations suggest using each aperture once and only once in order to avoid splitting the flux received on each aperture. Moreover, non-redundant configurations allow a broader spatial frequency coverage. We study aperture configurations based on these two conditions.

We describe this problematic formally and we apply results from combinatorial theory to prove the existence of solutions to some problems of aperture configuration optimization, and to exhibit some explicit solutions.

Firstly, we suggest new aperture configurations leading to a dense spatial frequency coverage. Secondly, we use these results to propose an optimal frequency coverage for a SPIDER-like design. Then, by complementing the latter instrument with a monolithic telescope, we propose a new aperture configuration that extends the spatial frequency coverage. Lastly, additional strategies to further extend the cut-off spatial frequency are explored and presented.

Keywords: Interferometry, combinatorial theory, frequency coverage optimization

Contents

Further author information:
E-mail: hiyam.debary@onera.fr, Telephone: +33 (0)1 46 73 47 60

1. INTRODUCTION

The innovative optical imaging system concept based on interferometry known as SPIDER could bring substantial gains in size and weight compared to a conventional focal plane imager. This compact interferometric imager uses both photonic integrated circuits and interferometric imaging technologies.

The so-called SPIDER demonstrator was initially presented by Lockheed Martin in 2013[1] and a couple experimental demonstrations followed.[2,3] Several aspects of such a concept have been studied since then.[4–8] In such a system, apertures are evenly disposed in one-dimensional arrays, called arms in the following. Each arm is associated with a PIC which combines apertures, used at most once, by pairs. The arms are disposed in a radial manner on a disc, as shown in Figure 2. The apertures within each arm collect light from a scene and inject it into an optical guide on a PIC chip. The light travels through various optical devices in the PIC, as represented in Figure 1.

The data measured by each detector pair, for a set of suitable values of the phase shifters, constitutes an interferogram. The main characteristics of the interferogram are the *contrast* and *position* of the fringes, which once grouped together form a physical quantity called the *complex visibility*.

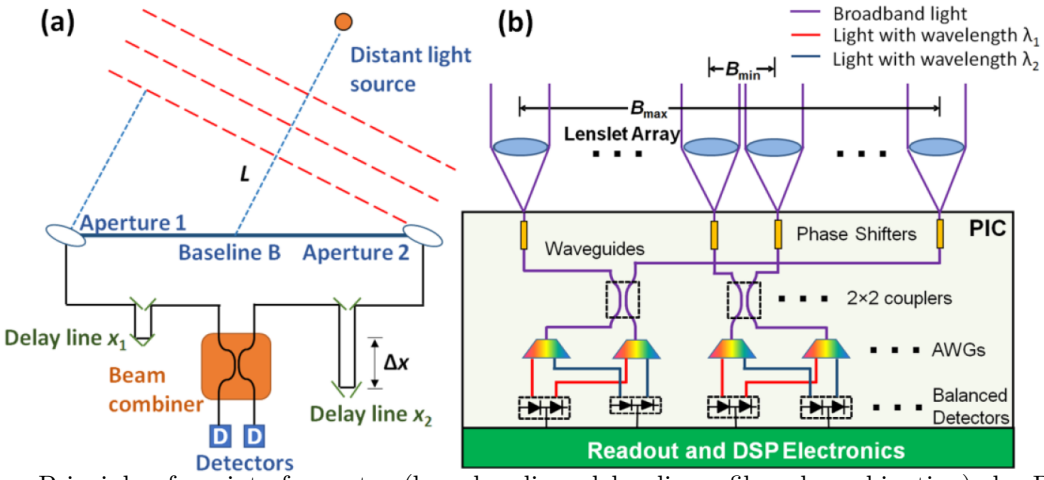

Figure 1: a: Principle of an interferometer (long baseline, delay lines, fibered combination); b: Principle of SPIDER (sub-aperture array, injection in a PIC that contains dispersing elements (AWGs), phase shifters, couplers (MMIs) and detectors).[9]

For each aperture pair separated by a distance called *baseline*, the measured complex visibility allows one to access one sample of the Fourier transform of the object using the Van Cittert-Zernike theorem. The sampled frequency is directly linked to the baseline of the aperture pair. The object can then be estimated through an image reconstruction, using the same methods as those developed in astronomical interferometry.[10,11]

In the following, we will refer to the set of measured spatial frequencies as the *frequency coverage*. It is a key aspect in the design of the interferometer, and should be tailored to the type of source observed.[12] In an interferometer similar to the one represented in Figure 2, the spatial frequencies are sampled with a step of b/λ,

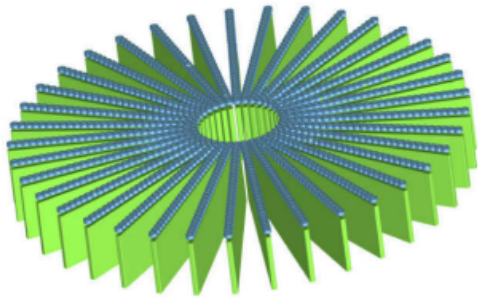

Figure 2: Schematic diagram of a compact interferometric imager.[9]

with b the distance between two consecutive apertures. In the following, for simplicity purposes, we will consider normalized spatial frequencies in units of b/λ.

We focus on the interferometric observation of a very extended source such as the Earth, viewed from a satellite. In this framework, Harvey and Rockwell[13] introduced the "practical resolution limit" (PRL), defining it as the maximum spatial frequency before which no zero occurs in the optical transfer function. Indeed, few priors are available for a very extended source, making it necessary to have no gaps in the frequency coverage. We qualify such a frequency coverage as compact.[14,15]

In the following, we will call an *aperture configuration* the list of combined aperture pairs in the instrument. Lockheed Martin's aperture configuration[16] is presented in the top panel of Figure 3. The frequency coverage associated to this aperture configuration is presented at the bottom, and each measured frequency is represented by a blue dot. What is noticeable is that not all apertures are used (the unused ones are shown in red) and that missing frequencies start from spatial frequency 7. Moreover, the higher the spatial frequencies, the more gaps there are.

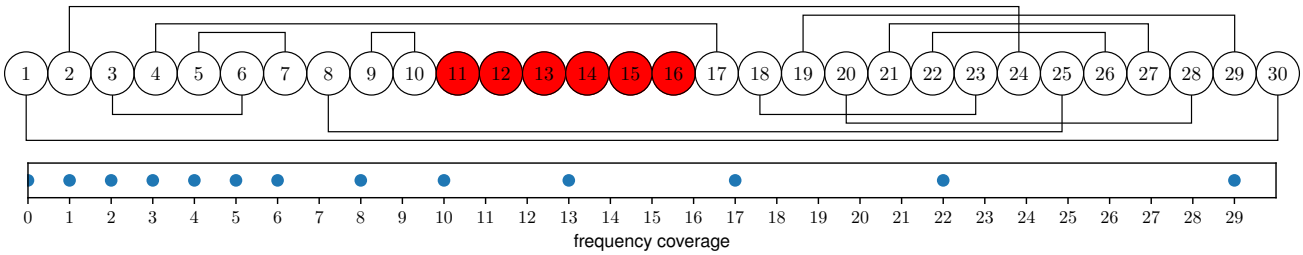

Figure 3: Top panel: aperture configuration of an interferometric arm of the SPIDER-like instrument as described in.[16] The black lines represent aperture pairings. The unused apertures are colored in red. Bottom panel: associated frequency coverage.

A different aperture configuration was suggested in[6,7,17] for the same SPIDER-like design with a frequency coverage producing only every other spatial frequency, and is presented at the top of Figure 4. In this case, all the apertures are used, but gaps are still observed as every other frequency is missing.

In the presented SPIDER-like designs, each arm has the same aperture configuration and consequently the same frequency coverage. Moreover, each measured frequency is unique. Finally, in both cases, there are gaps between frequencies. In order to reconstruct the missing frequencies in a satisfactory manner, strong priors on the object are required such as the knowledge that it has a reduced support on a dark background, as would be the case if observing various astronomical objects. Therefore, none of these aperture configurations are suitable for the observation of an extended source.

Apart from these designs, two other non radial architectures have been suggested in the literature. The first is a hexagonal array of apertures with a spiral pattern[18] providing a compact structure and a different frequency

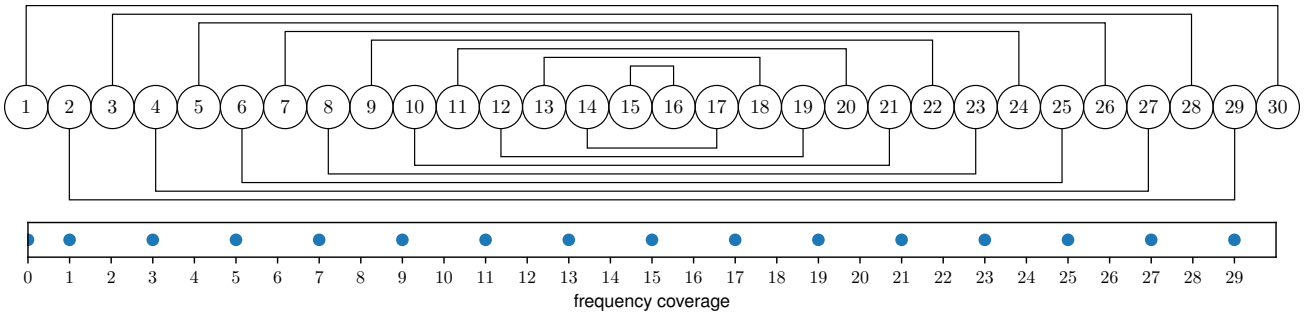

Figure 4: Top panel: aperture configuration of an interferometric arm of the SPIDER-like instrument as described in.[6,7,17] Bottom panel: associated frequency coverage.

coverage. This architecture necessitates in-development 2D PICs, thus excluding it from the scope of our study as we aim at using existing linear PICs. The second architecture involves a T-shape array of apertures and produces non simultaneous measurements.[19] In the following, as we consider snapshot instruments, this design is not appropriate.

2. OPTIMIZATION OF THE FREQUENCY COVERAGE OF DENSE 1D ARRAYS

In this communication, we aim at optimizing the frequency coverage of such a SPIDER-like interferometer replacing a traditional telescope.

The SPIDER-like instrument keeps *the same*:

- radially disposed interferometric arms as shown in Figure 2,
- aperture configuration shared between each arm,
- single use of each aperture,
- uniqueness of each measured spatial frequency (to avoid spatial frequency redundancy).

In contrast, we wish to use all apertures available in order to broaden the spatial frequency coverage, thus to maximise the PRL. Note that the novelty in our study is that the optimization is carried out among all the possible configurations, unlike previous authors,[7,17] without a costly systematic search.

The number of aperture configurations scales exponentially with the number of apertures, making it impossible to carry out a systematic exploration. For instance, for 40 apertures, there are 12521965697 different frequency coverages.[20] In this paper, we present an original approach based on combinatorial theory results obtained by several authors,[20–24] to solve the problem no matter the number of apertures, as well as to provide an explicit aperture configuration solution. Finally, this approach is applied to optimize such an instrument.

Considering each aperture used a single time and connected by pairs, the total number of apertures N_p is necessarily even. Moreover, the number of measured spatial frequencies is consequently $N_\mathsf{p}/2$ and the measured frequencies have values in the range $[1, N_\mathsf{p} - 1]$. We define a *buildable frequency coverage* as one that has an aperture configuration leading to it. It should be noted that not all frequency coverages are buildable. For the sake of the example, let us consider a frequency coverage of the form $\{\ldots, N_\mathsf{p} - 2, N_\mathsf{p} - 1\}$ that is trivially not buildable. Indeed, the two outer apertures have to be connected in order to measure the $N_\mathsf{p} - 1$ spatial frequency, leaving a next maximal measurable spatial frequency of $N_\mathsf{p} - 3$.

Here, we focus on finding buildable frequency coverages that have a *compact structure*, *i.e.* that are composed of consecutive spatial frequencies $\{1, 2, \ldots, N_\mathsf{p}/2\}$. This problem has been formulated and solved in the framework of combinatorial theory by Skolem,[21] and such a frequency coverage is called a Skolem set and its associated aperture configuration a Skolem sequence.

More generally, we wish to build frequency coverages in the form $\{n_{\mathsf{min}}, n_{\mathsf{min}}+1, \ldots, n_{\mathsf{min}}+N_{\mathsf{p}}/2-1\}$, where n_{min} is the first measured spatial frequency. This problem has been introduced by Langford,[25] and such a frequency coverage is called a Langford set and its associated aperture configuration a Langford sequence. The existence of buildable compact frequency coverages was solved for $n_{\mathsf{min}}=1$ by Skolem in 1958, for $n_{\mathsf{min}}=2$ by Davies[22] in 1959, then partially generalized by Bermond[23] in 1978 and finally completed by Simpson[24] in 1983.

To sum up the results derived by these authors: a frequency coverage of the form $\{n_{\mathsf{min}}, n_{\mathsf{min}}+1, \ldots, n_{\mathsf{min}}+N_{\mathsf{p}}/2-1\}$ is buildable if and only if :

$$4n_{\mathsf{min}} \leq N_{\mathsf{p}}+2 \tag{1}$$

yielding a condition on the highest minimum spatial frequency for n_{min}:

$$n_{\mathsf{min}} \leq \left\lfloor \frac{N_{\mathsf{p}}+2}{4} \right\rfloor \triangleq n_{\mathsf{min}}^{\mathsf{max}} \tag{2}$$

and any of:

- $N_{\mathsf{p}} \equiv 0 \pmod 8$,
- $N_{\mathsf{p}} \equiv 2 \pmod 8$ and n_{min} odd,
- $N_{\mathsf{p}} \equiv 6 \pmod 8$ and n_{min} even.

In other words, condition 1 translates into having a maximal first spatial frequency of $\frac{N_{\mathsf{p}}+2}{4}$ and consequently the highest spatial frequency of $\frac{3N_{\mathsf{p}}-2}{4}$. A single explicit aperture configuration is provided in[21–24] given the values of N_{p} and n_{min} defining the frequency coverage, as follows:

- $n_{\mathsf{min}}=1$:
  - $N_{\mathsf{p}} \equiv 0 \pmod 8$: see 1st part of proof of theorem 2[21]
  - $N_{\mathsf{p}} \equiv 2 \pmod 8$: see 2nd part of proof of theorem 2[21]
  - $N_{\mathsf{p}} \equiv 4 \pmod 8$: no solution[21]
  - $N_{\mathsf{p}} \equiv 6 \pmod 8$: no solution[21]
- $n_{\mathsf{min}}=2$:
  - $N_{\mathsf{p}} \equiv 0 \pmod 8$: see 1st part of proof of theorem 2[22]
  - $N_{\mathsf{p}} \equiv 2 \pmod 8$: no solution[22]
  - $N_{\mathsf{p}} \equiv 4 \pmod 8$: no solution[22]
  - $N_{\mathsf{p}} \equiv 6 \pmod 8$: see 2nd part of proof of theorem 2[22]
- $n_{\mathsf{min}}>2$:
  - $N_{\mathsf{p}} \equiv 0 \pmod 8$:
    - $n_{\mathsf{min}} \equiv 0 \pmod 4$: see 1st table of[24]
    - $n_{\mathsf{min}} \equiv 1 \pmod 4$: see 4th table of[24]
    - $n_{\mathsf{min}} \equiv 2 \pmod 4$: see 2nd table of[24]
    - $n_{\mathsf{min}} \equiv 3 \pmod 4$: see 3rd table of[24]
  - $N_{\mathsf{p}} \equiv 2 \pmod 8$:
    - $n_{\mathsf{min}} \equiv 0 \pmod 2$: no solution (as mentioned before)[23]
    - $n_{\mathsf{min}} \equiv 1 \pmod 2$: see 2nd table under theorem 2[23]
  - $N_{\mathsf{p}} \equiv 4 \pmod 8$: no solution (as mentioned before)[23]
  - $N_{\mathsf{p}} \equiv 6 \pmod 8$:
    - $n_{\mathsf{min}} \equiv 0 \pmod 2$: see 1st table under theorem 2[23]
    - $n_{\mathsf{min}} \equiv 1 \pmod 2$: no solution (as mentioned before)[23]

3. APPLICATION TO A SPIDER-LIKE INTERFEROMETER

In the Skolem configuration for the SPIDER-like interferometer, *i.e.* $n_{\mathsf{min}} = 1$, the measured spatial frequencies are $\{1, 2, \ldots, N_{\mathsf{p}}/2\}$ and thus the frequency coverage is buildable if and only if $N_{\mathsf{p}} \equiv 0$ or $2 \pmod 8$.

In this paragraph and applying the Skolem results, we propose a rewiring of the SPIDER-like instrument considered in order to increase the PRL. As $N_{\mathsf{p}} = 30$ does not satisfy the congruity condition given above, we consider the closest working case $N_{\mathsf{p}} = 32$. Using the constructive solution from the first half of the proof of theorem 2 in,[21] we provide an illustrative aperture configuration in Figure 5. In this configuration, the measured

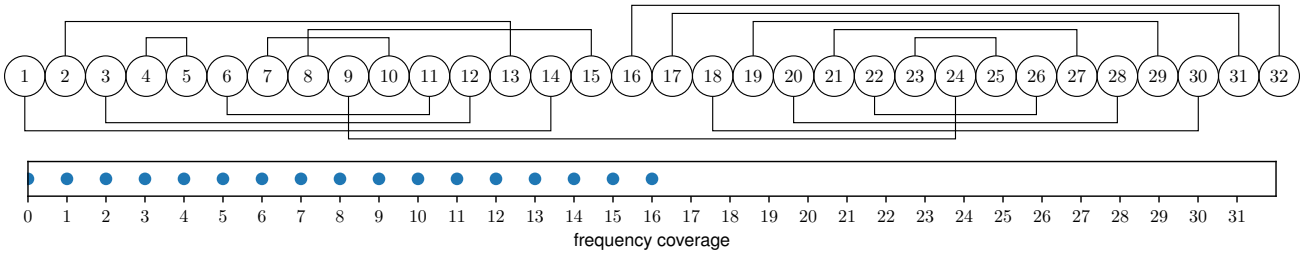

Figure 5: Top panel: example of a Skolem aperture configuration with 32 apertures. Bottom panel: the associated normalized frequency coverage ranging from 1 up to 16.

frequencies are $\{1, 2, 3, 4, 5, 6, 7, 8, 9, 10, 11, 12, 13, 14, 15, 16\}$.

In a nutshell, this aperture configuration achieves a compact frequency coverage in contrast to SPIDER, and improves the PRL as it is no longer equal to 6, but 16.

4. SUGGESTION OF A HYBRID ARCHITECTURE

4.1 Application case using Langford configurations

The second step of this paper consists in further optimizing the PRL obtained for the SPIDER-like design. To this aim, the design of a hybrid instrument constituted of the interferometer complemented with a small monolithic telescope measuring short spatial frequencies is considered.

To be more specific, we no longer wish to consider frequency coverages starting at the spatial frequency 1 but rather as high as possible considering the low spatial frequencies are measured by the monolithic telescope, to improve the resolution of the device. Note that if buildable, the Skolem configuration reaches a maximum spatial frequency of $N_{\mathsf{p}}/2$ by definition whereas the Langford configuration reaches a maximum spatial frequency of $(3N_{\mathsf{p}} - 2)/4$ as shown in Equation (2). Because the maximum spatial frequency measured increases from $N_{\mathsf{p}}/2$ to $(3N_{\mathsf{p}} - 2)/4$, the resolution of this hybrid interferometer is therefore improved by about 50% with respect to the interferometer with the Skolem configuration.

Maintaining the SPIDER-like interferometer aperture complexity, *i.e.* $N_{\mathsf{p}} = 30$ as presented in Figure 3, we apply these results and we aim at finding a compact frequency coverage with the highest minimum spatial frequency, $n_{\mathsf{min}}^{\mathsf{max}}$, as defined in Equation (2). A consequence of the latter is that $n_{\mathsf{min}}^{\mathsf{max}} = 8$ for $N_{\mathsf{p}} = 30$. Using the first table under theorem 2 in,[23] we provide an illustration of this Langford aperture configuration in Figure 6. The represented aperture configuration produces a compact frequency coverage ranging from spatial frequencies 8 to 22, improving the frequency coverage provided by a Skolem configuration, *i.e.* by considerably stretching the highest spatial frequency.

4.2 Dimensioning of the monolithic telescope

For the hybrid design, using the interferometric arms to measure the frequency coverage $\{n_{\mathsf{min}}^{\mathsf{max}}, \ldots, n_{\mathsf{min}}^{\mathsf{max}} + N_{\mathsf{p}}/2 - 1\}$, the monolithic telescope, of diameter D_{m}, needs to measure the continuous spectrum $[0, n_{\mathsf{min}}^{\mathsf{max}}]$. This condition translates into $D_{\mathsf{m}} = n_{\mathsf{min}}^{\mathsf{max}} b$.

However, we need to verify whether or not such a monolithic telescope fits in the empty space of diameter D_{in} at the center of the instrument, *i.e.* if $D_{\mathsf{m}} \leq D_{\mathsf{in}}$. To compute this inner diameter, we make additional assumptions about the arms:

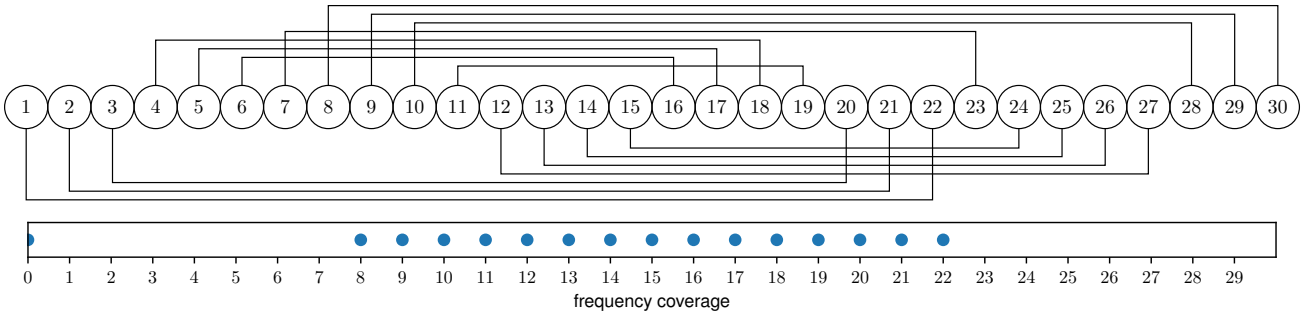

Figure 6: Top panel: example of a Langford configuration with 30 apertures. Bottom panel: the associated frequency coverage ranging from spatial frequency 8 up to 22.

1. the diameter of the apertures d, is equal to the distance between apertures b,
2. the arms of the interferometer are positioned in such a way that the apertures of the first ring are joint.

Considering these assumptions, the perimeter of the circle going through the center of each aperture $P = \pi(D_{\text{in}} + d)$ is larger than the perimeter of the regular polygon whose vertices are the centers of each aperture $P' = N_{\text{a}}d$, with N_{a} the number of interferometric arms. The inequality $P > P'$ translates into:

$$D_{\text{in}} > d(N_{\text{a}}/\pi - 1). \tag{3}$$

It is possible to rewrite this inequality into a condition on N_{a}, using the expression of the highest minimal spatial frequency of a Langford configuration $n_{\text{min}}^{\text{max}} = \lfloor (N_{\text{p}} + 2)/4 \rfloor$:

$$N_{\text{a}} \geq \pi \lfloor (N_{\text{p}} + 6)/4 \rfloor. \tag{4}$$

In the particular case of the SPIDER-like design with $N_{\text{a}} = 37$ and $N_{\text{p}} = 30$, we have $D_{\text{in}} > 10$ and $n_{\text{min}}^{\text{max}} = 8$. As a consequence, the condition allowing the monolithic telescope completing the missing low spatial frequencies of the Langford frequency coverage is verified. In contrast to SPIDER's frequency coverage presented in Figure 7a, all frequencies from 0 to 22 are measured whereas SPIDER has 11 missing frequencies in the range: $\{7, 9, 11, 12, 14, 15, 16, 18, 19, 20, 21\}$. This way, we have achieved a compact frequency coverage up to the spatial frequency 22 and in other words an improved PRL with respect to the SPIDER configuration.

In addition, Equation (4) suggests that we could maintain the same amount of apertures per arm while reducing the number of arms to 28 and still be able to achieve the same one-dimensional frequency coverage. This operation would reduce the total diameter of the instrument by reducing the inner space diameter. However it would be at the cost of having a less dense 2D frequency coverage.

Finally, in Figure 7b, we have represented the two-dimensional optical transfer function following the merging of the frequency coverages from the monolithic telescope and the SPIDER-like interferometer.

5. FURTHER INCREASE OF THE CUT-OFF FREQUENCY THROUGH ADDITIONAL ARMS

Previously, we have presented in Section 3, an optimization of the SPIDER-like design reaching a maximum frequency of $N_{\text{p}}/2$, using Skolem configurations. Then, in Section 4.2, we proposed a hybrid design reaching a maximum frequency of $(3N_{\text{p}} - 2)/4$, using Langford configurations complemented by a monolithic telescope. This section aims at proposing a new strategy to outperform both these frequency coverages and obtain a maximum measured frequency closer to $N_{\text{p}} - 1$, while maintaining the same diameter of the instrument. In order to do so, we plan on using the empty space between the interferometric arms visible in Figure 2.

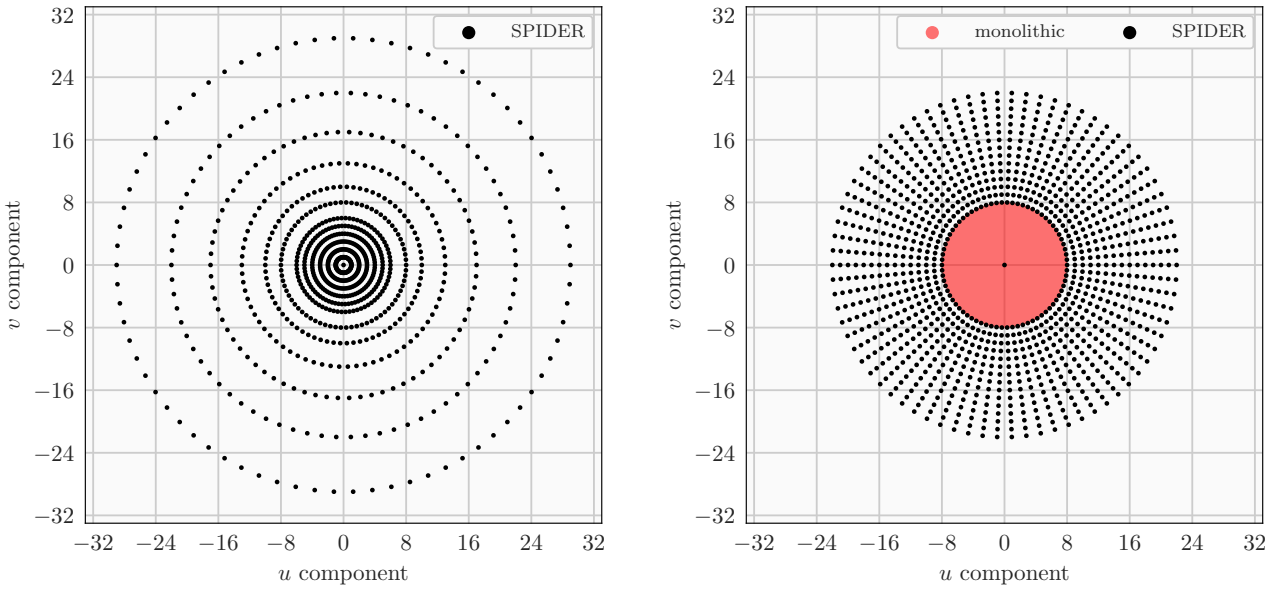

(a) (b)

Figure 7: a) Optical transfer function of the SPIDER-like instrument with radially disposed arms. Each interferometric arm measures the discrete spatial frequencies $\{1, 2, 3, 4, 5, 6, 8, 10, 13, 17, 22, 29\}$ (black). b) Optical transfer function of the suggested hybrid instrument with a monolithic telescope complemented by a SPIDER-like instrument with radially disposed arms. The monolithic measures the continuous spatial frequencies $[1, 8]$ (red) and the interferometer the discrete spatial frequencies $\{8, \ldots, 22\}$ (black).) from Section 4.2.

5.1 Optimizing the inter-arm empty space: dimensioning the additional arms

The empty space between the set of interferometric arms, called *primary arms*, can allow the installation of another set of shorter arms, called *secondary arms*, as presented in Figure 8. This section aims at determining their size.

Knowing the diameter d of the apertures and the small angle $\alpha = 2\pi/N_{\mathsf{a}}$ separating two arms, we can compute the distance R allowing to install the first aperture of the secondary arm as:

$$R = \frac{d/2}{\tan(\alpha/2)} \approx \frac{dN_{\mathsf{a}}}{2\pi} \tag{5}$$

Let N_{p} be the number of apertures in the primary arm. Using Equation (5), the number of apertures of the secondary arm, $N_{\mathsf{p}}^{\mathsf{s}}$, writes:

$$N_{\mathsf{p}}^{\mathsf{s}} = N_{\mathsf{p}} - \left\lceil \frac{N_{\mathsf{a}}}{2\pi} \right\rceil \tag{6}$$

Thus, the secondary arms are $\lceil \frac{N_{\mathsf{a}}}{2\pi} \rceil$ apertures smaller than the primary arms and can also be disposed in a radial manner as shown in Figure 8b. Please note that since the number of primary arms is odd, each secondary arm is parallel to a primary arm on the opposite side of the instrument. The configurations we present in this section consider each pair of parallel primary and secondary arms.

Similarly to the analysis carried out in Section 2, we can focus on the one-dimensional optimization of the primary and secondary arms wiring, and replicate the same aperture configuration on each radially disposed pair of parallel primary and secondary arms.

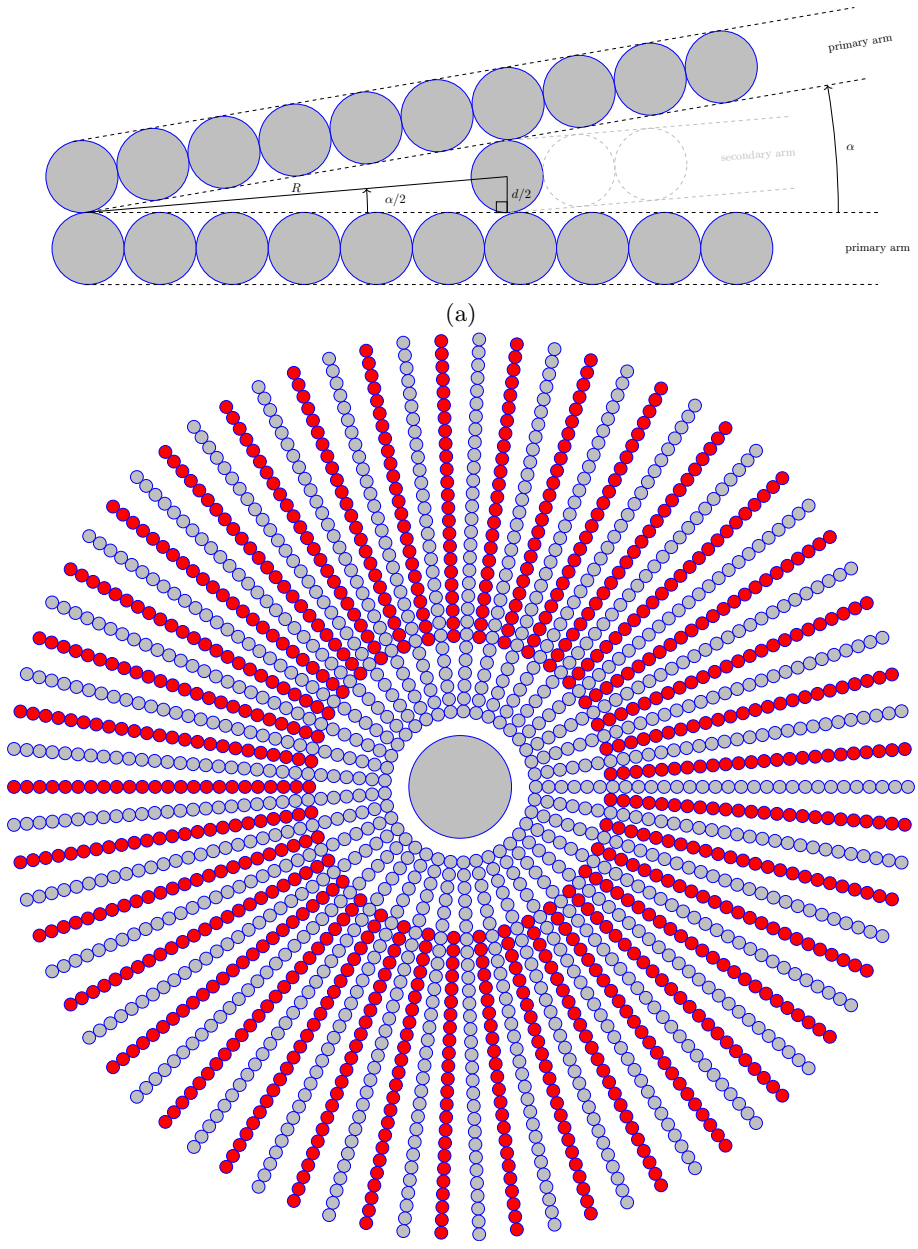

(a)

(b)

Figure 8: a) Schematic of the primary arms and the empty space allowing the installation of secondary arms. d is the diameter of an aperture, α the angle between two adjacent primary arms, and R the distance between the tangency point of the first aperture of two adjacent primary arms and the first aperture of the secondary arm that can be placed between them. b) Schematic of the hybrid instrument with the primary (in blue) and secondary arms (in red) complemented by the monolithic telescope (in gray) from Section 4.2.

5.2 Trivial baseline matching method the primary and secondary arms

The simplest approach to wiring both the primary and secondary arms is to measure all odd baselines within the secondary arm, and all even baselines within the primary arm. The wiring corresponding to measuring all odd spatial frequencies has already been presented in Figure 4, and the one corresponding to measuring all even spatial frequencies is identical, with an unused aperture in the middle, incrementing all measured spatial frequencies by

a unity. More specifically, using the described method, and assuming N_p and N_p^s to be even, it is possible for the primary arm to measure $\{2, 4, \ldots, N_\mathsf{p} - 2\}$, and for the secondary arm to measure $\{1, 3, \ldots, N_\mathsf{p}^\mathsf{s} - 1\}$. This trivial configuration is dense up to N_p^s, as $N_\mathsf{p}^\mathsf{s} + 1$ is the first missing baseline.

5.3 An iterative baseline matching method for wiring primary and secondary arms

In this subsection, we aim at presenting a method to wire the apertures of two types of primary and secondary arms in order to reach the highest maximum frequency possible. The method is composed of an iterative step that is applied alternatively to the primary and secondary arms. We will consider the general case:

$$N_\mathsf{p} = N_\mathsf{p}^\mathsf{s} + \Delta_\mathsf{p}, \tag{7}$$

with an odd difference between the primary and secondary arms $\Delta_\mathsf{p} = 2k + 1$.

Here we aim at explicitly showing how to wire any consecutive $N \geq 2\Delta_\mathsf{p}$ apertures, in a way to measure the Δ_p consecutive baselines $\{N - 3k - 1, N - 3k, \ldots, N - k - 1\}$, and leaving $N - 2\Delta_\mathsf{p} = N - 4k - 2$ consecutive unused apertures (in the center of Figure 9). A figure representing the associated baseline pairing is presented in Figure 9.

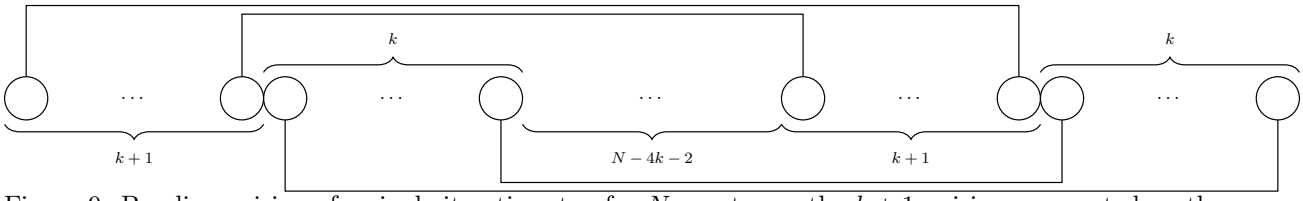

Figure 9: Baseline pairing of a single iterative step for N apertures: the $k + 1$ pairings connected on the upper part of the figure are $\{N - 3k - 1, N - 3k + 1, \ldots, N - k - 1\}$ and the k pairings connected on the lower part of the figure are $\{N - 3k, N - 3k + 2, \ldots, N - k - 2\}$. The union of these sequences is the compact frequency coverage $\{N - 3k - 1, N - 3k, \ldots, N - k - 1\}$.

Applying this step alternatively on the primary and secondary arms yields:

1. **wiring to primary arm with** $N = N_\mathsf{p}$: measures $\{N_\mathsf{p} - 3k - 1, N_\mathsf{p} - 3k, \ldots, N_\mathsf{p} - k - 1\}$, leaving $N_\mathsf{p} - 2\Delta_\mathsf{p}$ consecutive unused apertures on the primary arm,
2. **wiring to secondary arm with** $N = N_\mathsf{p}^\mathsf{s} = N_\mathsf{p} - \Delta_\mathsf{p}$: measures $\{N_\mathsf{p} - 5k - 2, N_\mathsf{p} - 5k - 1, \ldots, N_\mathsf{p} - 3k - 2\}$, leaving $N_\mathsf{p} - 3\Delta_\mathsf{p}$ consecutive unused apertures on the secondary arm,
3. **wiring to primary arm with** $N = N_\mathsf{p} - 2\Delta_\mathsf{p}$: measures $\{N_\mathsf{p} - 7k - 3, N_\mathsf{p} - 7k - 2, \ldots, N_\mathsf{p} - 5k - 3\}$, leaving $N_\mathsf{p} - 4\Delta_\mathsf{p}$ consecutive unused apertures on the primary arm,
4. ***etc.***

This way, we can see that by construction, our iterative pairing method forms a compact frequency coverage with a maximum measured frequency of $N_\mathsf{p} - (\Delta_\mathsf{p} - 1)/2 - 1 \simeq N_\mathsf{p} - 1 - N_\mathsf{a}/(2\pi)$. In the particular case where $N_\mathsf{p} \equiv 0 \pmod{\Delta_\mathsf{p}}$, the frequency coverage is dense from $k + 1$ to $N_\mathsf{p} - k - 1$. Please note that for this method to yield a compact frequency coverage, it is key for the number of apertures paired at each step to be identical to the differences between primary and secondary arms. This kind of setup, combined with the use of a monolithic telescope measuring the low frequencies as presented in Section 4.2, outperforms the trivial frequency coverage presented in Section 5.2 in the sense that it achieves a higher compact frequency coverage. More specifically, in the favorable setup for the trivial baseline pairing method *i.e.* with N_p^s even, the cut-off spatial frequency is of N_p^s whereas in the presented method, we reach a cut-off spatial frequency of $N_\mathsf{p} - k - 1 = N_\mathsf{p} - (2k + 1) + k = N_\mathsf{p}^\mathsf{s} + k$.

5.4 Application to the studied SPIDER-like design

As shown in Section 5.1, the number of arms considered enforces a certain difference in the number of apertures between the primary and secondary arms. In the case where $N_\mathsf{p} = 30$, $d = 1$ and $N_\mathsf{a} = 37$, using Equation (6), this difference is of 6. This number being incompatible with the general method we presented in Section 5.3, it is however possible to adapt our general method to this application, simply by having a different initial wiring for the primary arm: as presented in Figure 10, it is possible to wire any consecutive $N \geq 13$ apertures, in a way to measure the 6 consecutive baselines $\{N-9, N-8, \ldots, N-4\}$, and leaving $N-13$ consecutive unused apertures as well as a non-contiguous unused aperture. By initially applying this baseline matching method to

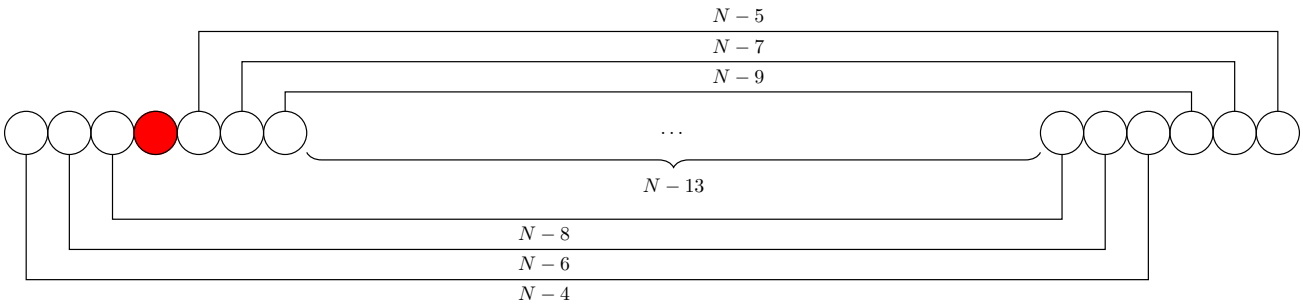

Figure 10: Diagram representing the initial pairing method for the primary arm. The first 6 consecutive baselines measured are $\{N-9, N-8, \ldots, N-4\}$. The unused aperture is represented in red. The remaining $N-13$ unused consecutive apertures are represented by the dots in the middle.

the primary arm with $N = N_\mathsf{p}$ leaves us with $N_\mathsf{p} - 13$ consecutive unused apertures on the primary arm, and $N_\mathsf{p}^\mathsf{s} = N_\mathsf{p} - 6$ on the secondary arm. It is now possible to apply alternatively the general method presented in Section 5.3 with $\Delta_\mathsf{p} = 7$.

An illustrative application of the step-by-step of the baseline matching of the interferometric arms is presented in Figure 11. Once the condition $N \geq 2\Delta_\mathsf{p}$ is not met, we manually wire the remaining unused apertures (bottom two panels).

To sum up, we have showed how to measure all frequencies, $\{1, 2, \ldots, 26\}$ without gaps from two arms containing respectively 30 and 24 apertures. This maximal value 26 is larger than the solution by Skolem and Langford and does not even necessitate the use of a monolithic telescope to measure the low frequencies. With this new method, we achieve a radial frequency coverage of almost 90% (vs. 50% and 75% achieved by respectively the Skolem and Langford configurations), without modifying the size of the instrument.

6. CONCLUSION

In summary, we have proposed an original method allowing one to determine whether or not a compact frequency coverage is buildable, given the number of apertures and the lowest sought spatial frequency. The solution is constructive and does not require a computationally costly systematic exploration, making our approach fit to interferometric arms with a large number of apertures. This tool allowed us firstly to propose a rewiring of the SPIDER architecture, achieving a compact frequency coverage. We then used it to suggest a hybrid architecture combining a small monolithic telescope, for low spatial frequency measurements, placed at the center of a SPIDER-like instrument that measures higher spatial frequencies and still achieves a compact frequency coverage. These results were recently accepted for publication in a peer-reviewed journal.[12] Finally, a new method has been proposed allowing one to further increase the cut-off frequency, and can be applied whatever the number of apertures. A current limitation of the frequency coverage work presented here is that it only considers radial frequencies. A perspective of this work is thus to consider the 2D frequency coverage and fill in the gaps azimuthally.

ACKNOWLEDGMENTS

The PhD of HD is funded by Airbus Defence & Space and ONERA.

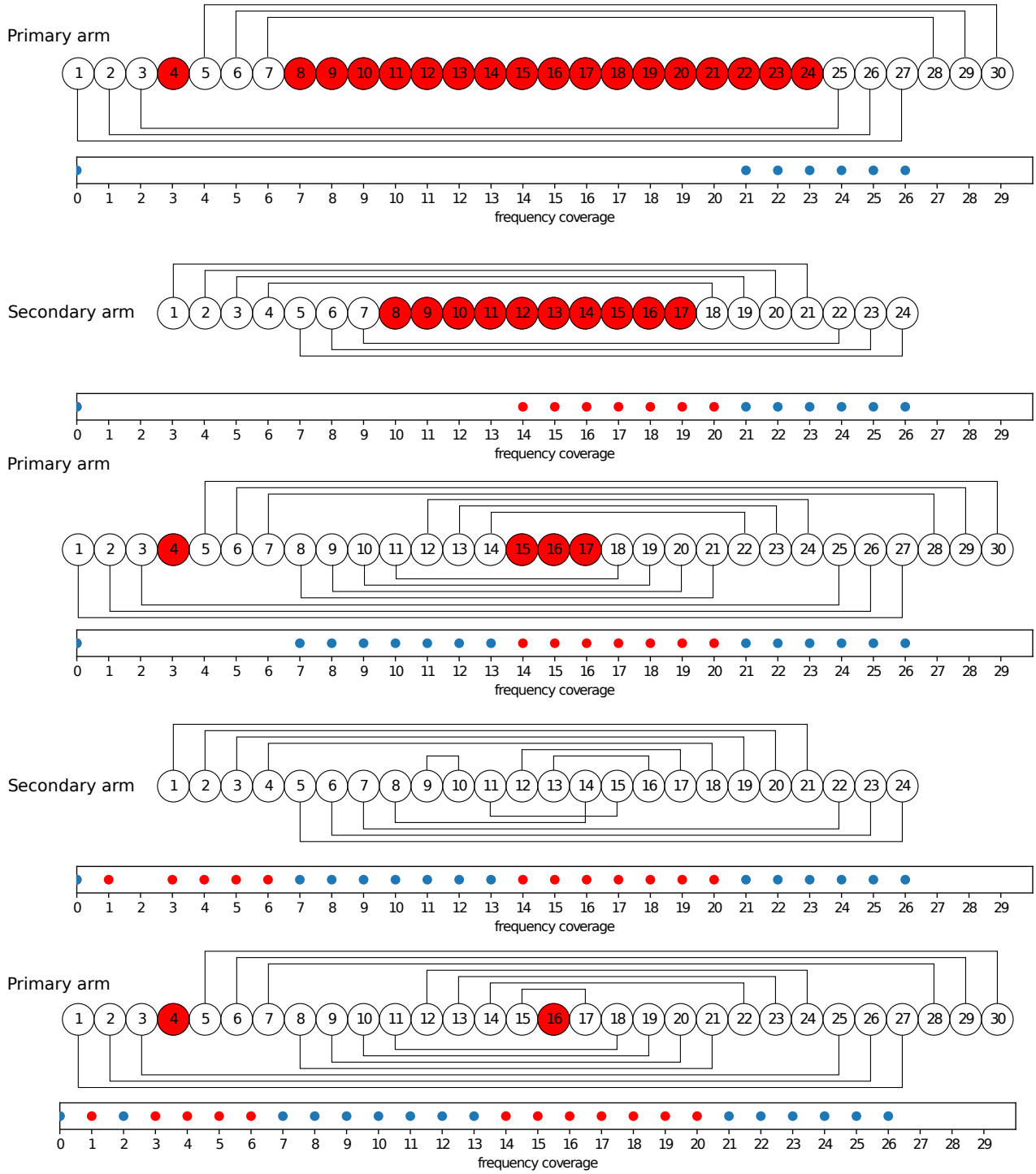

Figure 11: Diagram representing the aperture configurations and associated frequency coverages for the initial and general pairing methods with both the primary and secondary arms. Unused apertures are represented in red and the frequency coverages at each step are cumulative. The frequencies measured by the primary arm are represented in red and those measured by the secondary arm are represented in blue.

REFERENCES

[1] Kendrick, R. L., Duncan, A., Ogden, C., Wilm, J., Stubbs, D. M., Thurman, S. T., Su, T., Scott, R. P., and Yoo, S., "Flat-panel space-based space surveillance sensor," in [*Advanced maui optical and space surveillance technologies conference*], E45 (2013).

[2] Scott, R. P., Su, T., Ogden, C., Thurman, S. T., Kendrick, R. L., Duncan, A., Yu, R., and Yoo, S., "Demonstration of a photonic integrated circuit for multi-baseline interferometric imaging," in [*2014 IEEE Photonics Conference*], 1–2, IEEE (2014).

[3] Su, T., Scott, R. P., Ogden, C., Thurman, S. T., Kendrick, R. L., Duncan, A., Yu, R., and Yoo, S., "Experimental demonstration of interferometric imaging using photonic integrated circuits," *Optics Express* **25**(11), 12653–12665 (2017).

[4] Liu, G., Wen, D.-S., and Song, Z.-X., "System design of an optical interferometer based on compressive sensing," *Monthly Notices of the Royal Astronomical Society* **478**(2), 2065–2073 (2018).

[5] Gao, W., Wang, X., Ma, L., and Guo, D., "Quantitative analysis of imaging quality of the segmented planar imaging detector," in [*Tenth International Conference on Information Optics and Photonics*], **10964**, 633–641, SPIE (2018).

[6] Guo-mian, L., Qi, L., Yue-ting, C., Hua-jun, F., Zhi-hai, X., and Jingjing, M., "An improved scheme and numerical simulation of segmented planar imaging detector for electro-optical reconnaissance," *Optical Review* **26**(6), 664–675 (2019).

[7] Cao, K., Ye, Z., Jiang, C., Zhu, J., Qiao, Z., and Jiang, Y., "Lenslets combination optimal design of the segmented planar image detector for electro-optical reconnaissance," *Optical Engineering* **59**(4), 043105 (2020).

[8] Liu, G., Wen, D., Song, Z., and Jiang, T., "System design of an optical interferometer based on compressive sensing: an update," *Optics Express* **28**(13), 19349–19361 (2020).

[9] Su, T., Liu, G., Badham, K. E., Thurman, S. T., Kendrick, R. L., Duncan, A., Wuchenich, D., Ogden, C., Chriqui, G., Feng, S., Chun, J., Lai, W., and Yoo, S. J. B., "Interferometric imaging using si3n4 photonic integrated circuits for a spider imager," *Opt. Express* **26**, 12801–12812 (May 2018).

[10] Le Besnerais, G., Lacour, S., Mugnier, L. M., Thiébaut, E., Perrin, G., and Meimon, S., "Advanced imaging methods for long-baseline optical interferometry," *IEEE Journal of Selected Topics in Signal Processing* **2**(5), 767–780 (2008).

[11] Thiébaut, É. and Young, J., "Principles of image reconstruction in optical interferometry: tutorial," *JOSA A* **34**(6), 904–923 (2017).

[12] Debary, H., Mugnier, L. M., and Michau, V., "Aperture configuration optimization for extended scene observation by an interferometric telescope," *Optics Letters* **accepted** (2022).

[13] Harvey, J. E. and Rockwell, R. A., "Performance characteristics of phased array and thinned aperture optical telescopes," *Optical Engineering* **27**(9), 279762 (1988).

[14] Damé, L. and Martic, M., "Study of an optimized configuration for interferometric imaging of complex and extended solar structures.," *Targets for Space-Based Interferometry* **354**, 201–208 (1992).

[15] Mugnier, L. M., Rousset, G., and Cassaing, F., "Aperture configuration optimality criterion for phased arrays of optical telescopes," *J. Opt. Soc. Am. A* **13**, 2367–2374 (Dec 1996).

[16] Badham, K., Kendrick, R. L., Wuchenich, D., Ogden, C., Chriqui, G., Duncan, A., Thurman, S. T., Yoo, S. J. B., Su, T., Lai, W., Chun, J., Li, S., and Liu, G., "Photonic integrated circuit-based imaging system for spider," in [*2017 Conference on Lasers and Electro-Optics Pacific Rim (CLEO-PR)*], 1–5 (2017).

[17] Chu, Q., Shen, Y., Yuan, M., and Gong, M., "Numerical simulation and optimal design of segmented planar imaging detector for electro-optical reconnaissance," *Optics Communications* **405**, 288–296 (2017).

[18] Ding, C., Zhang, X., Liu, X., Meng, H., and Xu, M., "Structure design and image reconstruction of hexagonal-array photonics integrated interference imaging system," *IEEE Access* **8**, 139396–139403 (2020).

[19] Liu, G., Wen, D., Fan, W., Song, Z., Li, B., and Jiang, T., "Single photonic integrated circuit imaging system with a 2d lens array arrangement," *Opt. Express* **30**, 4905–4918 (Feb 2022).

[20] Nordh, G., "Perfect skolem sets," *Discrete mathematics* **308**(9), 1653–1664 (2008).

[21] Skolem, T., "Some remarks on the triple systems of steiner," *Mathematica Scandinavica* **6**(2), 273–280 (1958).

[22] Davies, R. O., "On langford's problem (ii)," *The Mathematical Gazette* **43**(346), 253–255 (1959).

[23] Bermond, J.-C., Brouwer, A. E., and Germa, A., "Systemes de triplets et differences associees," in [*Probèmes combinatoires et théorie des graphes, Colloque international CNRS 260*], **260**, 35–38, CNRS (1978).
[24] Simpson, J. E., "Langford sequences: perfect and hooked," *Discrete Mathematics* **44**(1), 97–104 (1983).
[25] Langford, C. D., "Langford problem," *Math. Gazette* **42**, 228 (1958).